

# An Analysis of the Partial Discharge Pattern Related to the Artificial Defects Introduced at the Interface in an XLPE Cable Joint using a Laboratory Model

Jeon-Seon Lee and Ja-Yoon Koo

**Abstract** - In this work, in order to realize the possible defects at the cable joint interface, four different types of artificial defects are provided : conducting, insulating substances, void and scratches. The analysis related to the PD patterns has been performed by means of conventional Phase Resolved Partial Discharge Analysis (PRPDA) and Chaotic Analysis of Partial Discharge (CAPD) as well which was proposed by our previous communication. As a result, it could be pointed out that each defect has shown particular characteristics in its pattern respectively and that the nature of defect causing partial discharge could be identified more distinctively when the CAPD is combined with the conventional statistic method, PRPDA.

**Keywords** : PRPDA, CAPD, partial discharge

## 1. Introduction

Even though the cable joint splicing is performed very carefully by skillful technicians usually in manholes, various types of contaminants could be easily introduced at the interfaces, and thus, interfaces in the cable joint have been considered to be the weakest part of the extruded transmission power cable system [1]. According to the paper of CIGRE SC 15, when the electric stresses due to these interfacial defects are excessive, the partial discharges are known to be produced resulting in the interfacial electrical tree giving rise to eventually sudden breakdown [2]. On that account, partial discharge detection is suggested as one of the most effective means to the diagnosis of interfacial aging of joints.

Other precedent works have been carried out for the investigation on the nature of defects and the degree of degradation based on the PD measurement [3]. However, they might have faced some technical inconveniences related to the sensors associated with their measuring system. Moreover, the on-site applicability seems not to be so high since the transmission characteristics of PD pulse is affected by various parameters in connection with the cable accessories and PD signal transmission path [4]. In particular, many investigations on the PD pattern analysis have been reported by means of PRPDA using different types of defects, of which the results are consistent with each other only for the case of void.

In this respect, it is preferable not only to identify the nature of possible defects but also to obtain information about the present state of degradation of XLPE cable joints by recognizing their PD patterns. For this purpose, in order to realize the possible defects at the cable joint interface, four different types of artificial defects are introduced into our test specimen: conducting, insulating substances, void and scratches. And the analysis related to their PD patterns has been performed by means of the conventional Phase Resolved Partial Discharge Analysis (PRPDA) and Chaotic Analysis of Partial Discharge (CAPD).

The reason why the CAPD is proposed in this paper can be described from the two view points described in our previous communication [5]. Firstly, with respect to the PD occurrence in insulating material, space charges remaining near the defects, where the previous discharges have taken place, are considered to affect the generation of the following discharges. Therefore, the successive pulses should be investigated based on the effect of the previous discharges [7]. For this reason, mutual influences between consecutive pulses should be considered especially in the early stage of insulation aging, where space charges play a decisive role. In conventional PRPDA method, since the pulses are superimposed within finitely fixed phase windows of the applied voltage it could be remarked that information about the influences of the previous discharges could hardly be deduced [5]. Secondly, PD phenomena are suggested to be regarded as one of the deterministic dynamic processes where PD should occur under such assumption that the local electric field to be reached be sufficiently high.

And thus, its mathematical model can be described by either difference equations or nonlinear differential equations by use of several state variables that are obtained

---

This research was supported by Research Center for Electronic Materials & Components (EM&C) and LG Cable co. Ltd, KOREA.

Manuscript received: Aug. 28, 2002 accepted: Oct. 14, 2002

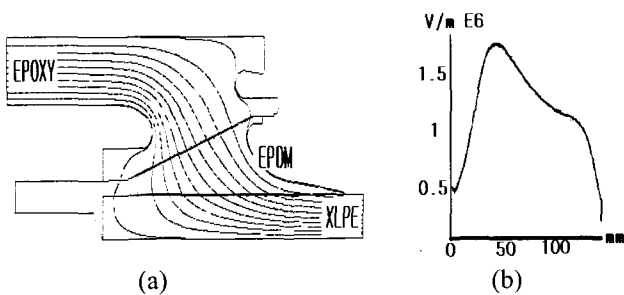
Jeon-seon Lee and Ja-yoon Koo are with School of Electric Engineering, Hanyang university and EM&C, Korea.

from the time sequential measured data of PD signals. These variables can provide the rich and complex behavior of detectable time series, for which Chaos theory can be employed.

## 2. Experiments

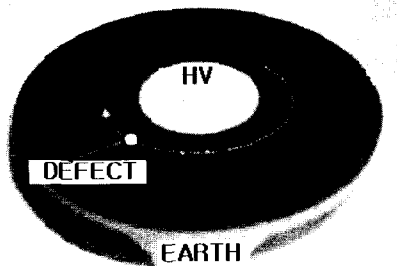
### 2.1 Test specimen modeling the XLPE cable joint

Fig. 1 shows the distribution of equipotential lines and electric stress in the cross-section of the interfaces of the prefabricated 154kV transmission cable joint. The equipotential distribution lines are normal to the EPOXY-EPDM rubber interface as shown in Fig. 1(a). The evolution of the tangential component of the electric field along the interface between EPDM-EPOXY is shown in Fig. 1(b), where the maximum electric field was calculated to be 1.8 kV/mm for the rating voltage at 154 kV.



**Fig. 1** Prefabricated joint and EPDM-EPOXY interface : (a) a distribution of equipotential line (b) the evolution of the tangential component of the electric field along the interface

The laboratory test sample, shown in Fig. 2, has been designed to maintain the electric field distributions in the same way as those of real cable joints as shown in Fig. 1.



**Fig. 2** Test sample for the investigation at the interfaces

In Fig. 3(b), the evolution of the tangential component of the electric field along the interface of our sample shows a similar aspect to that in Fig. 1(b).

This sample allows us to realize the experiments up to 70kV with various test parameters such as mechanical pressure, the presence of lubricant and the different natures

of the artificial defects.

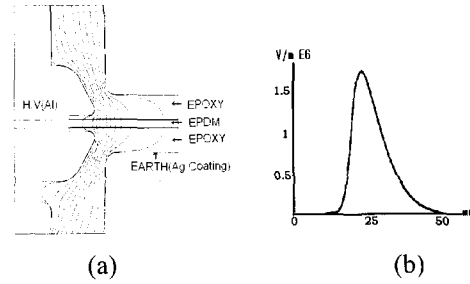


**Fig. 3** Laboratory test sample as the model of EPDM-EPOXY interface : (a) a distribution of equipotential line (b) the evolution of the tangential component of the electric field along the interface from the center of the sample

### 2.2 Experimental Setup

Fig. 4 shows the block diagram of the experimental setup. In this work, the HFPD detection method was applied for partial discharge measurement by use of CT of which the frequency band ranges from 2MHz to 100MHz, since easy on-site application of HFPD is well reported with appreciable success [6]. PD signals detected through CT have been measured in two different ways: a commercialized HFPD detecting system for the PRPDA and digital oscilloscope for the CAPD. Every 2 minutes, their information has been stored for every voltage application. Test voltage was applied in different ways depending on the purpose of the tests: For the measurement of the electric stress for PD, applied voltage was increased every 15 minutes with the step of  $1/2 E_{max}$  and for the analysis of PD pattern, a constant voltage was applied until breakdown.

For this work, it should be pointed out that the calculated electric field could reach its maximum “ $E_{max}$ ” of 1.8kV/mm under the applied voltage of 16 kV at all the points located on the circle of which the radius is 24mm from the center of the specimen as shown in Fig. 3(b). i.e., 16 kV corresponds to  $E_{max}$ . And various artificial defects introduced into the specimen in table 1 are placed at any point in this circle.

**Table 1** Artificial defects introduced at the interface

Defect	Description	Size( $\mu\text{m}$ )
Conducting particle	Copper wire	D=250, 500, 1000 L=1000
Void	Cylindrical void	D=250, 500, 1000 H=500
Insulating fiber	Cotton fiber soaked with water	L=5mm, $\Phi$ =100
Scratch	Scratch using sand paper(#400)	L=10mm

D: diameter, L: length, H: height

At the interface in the test sample, the applied mechanical pressure was fixed to be  $5\text{kgf/cm}^2$  and the lubricant was

not coated in order to avoid its dry-out remaining solid filler since lubricants are reported to remain at least for several weeks. [6]

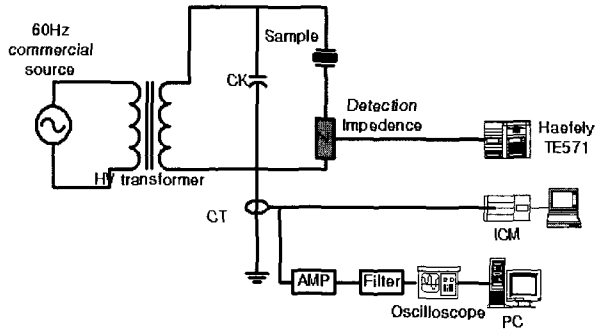


Fig. 4 Experimental setup

### 3. Results and Discussion

#### 3.1 Electric Stress for Partial Discharge

In this work, it could be suggested empirically to classify the aspect of partial discharge occurrence into two groups :  $PD_{GAP}$  and  $PD_{ET}$  for the interfacial defects. The former seems to take place at the voids or air gaps near the introduced contaminated particles causing eventually the electrical treeing. The latter might be produced during the propagation of electrical treeing at the interface in the specimen, which likely enhances the breakdown along the interface sooner or later. These two types of partial discharge can be distinguished by the evolution of partial discharge magnitude as a function of time under voltage application as follows. As shown in Fig. 5(a), the increase in the magnitude of the former is very slow, whereas unexpected sudden increase in the magnitude of the latter was observed as shown in Fig. 5(b) considering its time scale.

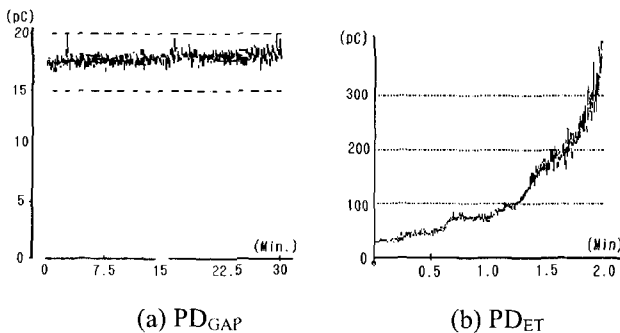
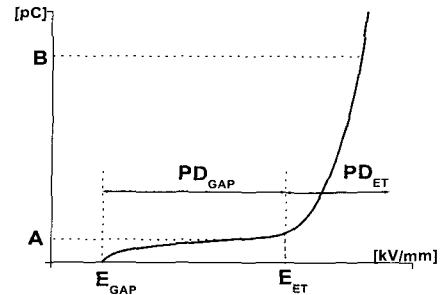


Fig. 5 Evolution of PD magnitude as a function of applied time

For this study, it should be emphasized that the intensity of electric stress giving rise to a different type of PD is probably the most important parameter to be considered. Therefore, Fig. 6 describes the fundamental conception by the schematic representation.

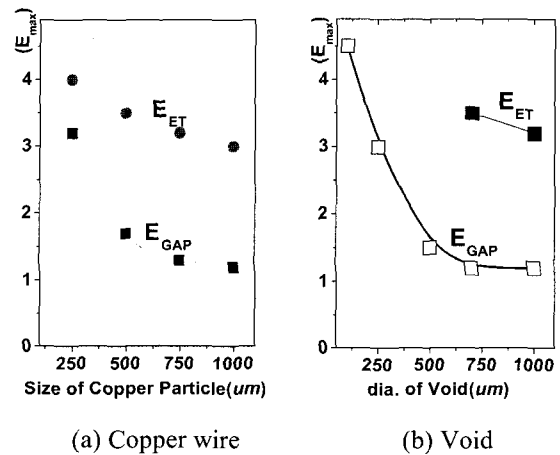


A : order of 10pC B : order of 100 pC  
 $E_{GAP}$ : Electric stress measured the magnitude of PD exceeding 5pC  
 $E_{ET}$ : Electric stress occurring sudden increase of the magnitude of PD

Fig. 6 The schematic representation of the intensity of electric stress giving rise to a different type of PD

In this Fig, the electric stress " $E_{GAP}$ ", corresponding to  $PD_{GAP}$ , has been measured and taken into account where the magnitude of PD exceeds 5pC which is the maximum acceptable PD for the qualification test at the manufactures. In the case of the latter, electric stress " $E_{ET}$ " corresponding to  $PD_{ET}$  has been taken as a parameter where the evolution of the PD displays the sudden increase in its magnitude.

Fig. 7 shows the dependence of the electric stress for PD on the dimension of the different nature of defects introduced at the interface in laboratory samples such as copper and void. Both  $E_{GAP}$  and  $E_{ET}$  are lowered ranging from over 4  $E_{max}$  to 1  $E_{max}$  with the increase in the dimension of the defects.



(a) Copper wire (b) Void  
 Fig. 7 Dependence of the electric stress for PD on the dimension of the defects

Fig. 8 shows the evaluation of the PD magnitude as a function of applied electrical stress due to defects such as the scratch and the insulating substances, where a sudden increase in their magnitudes is observed for both cases. This result may imply that the interfacial electrical tree could be formed directly from these two types of defects without forming any gaps.

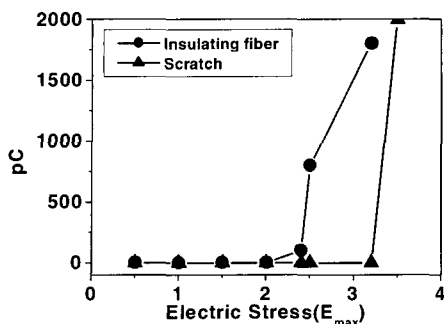


Fig. 8 Evolution of the PD magnitude as a function of applied voltage

### 3.2 PD pattern of the defect by phase resolved partial discharge analysis (PRPDA)

#### 3.2.1 Conducting particle

Fig. 9(a) shows  $\Phi$ -q-n patterns for the conducting particle, for which the ear of rabbit becomes longer with the sharp edged metal particle. After 12 hours' test, as shown in Fig. 9(b), the shape of the patterns at the period of 1/4 and 3/4 was transformed by the additional partial discharges generated possibly from the electrical treeing. It should be remarked that Fig. 9(c) is the typical PD pattern due to the electrical tree, which is clearly also revealed during our test. These two Figs might imply that the source generating PD is well altered from the voids to interfacial electrical treeing with the lap of testing time under voltage application. Besides, this suggestion could be proved by the increase of PD ranging from 100 pC to 500 pC within only 30 minutes. Afterwards, a slow increase in its magnitude was detected with time. As can be seen in Fig. 9(d), severe degradation was observed at the sharp edge of the metallic particle from which an interfacial electrical treeing has taken place.

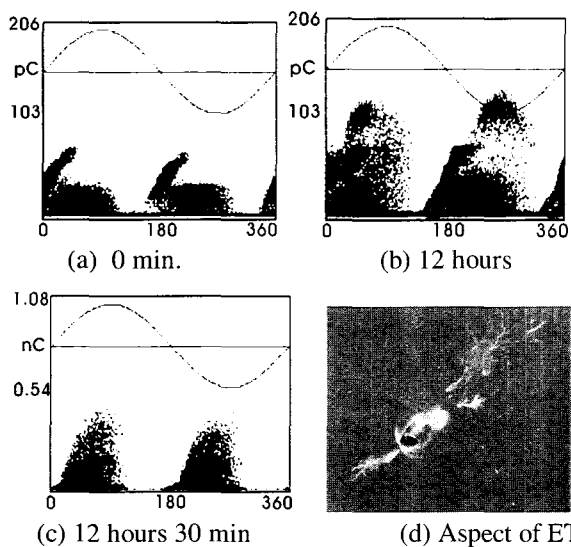


Fig. 9 Evolution of PD pattern for the conducting particle (copper) without silicone oil at  $2 E_{max}$ .

#### 3.2.2 Void

In this work, similar results to those of other experimental investigations have also been found with voids. Fig. 10(a) shows the typical partial discharge pattern from a single void prior to the formation of an electrical tree. It is also found that the partial discharge might be extinguished after the long period of voltage application. This phenomenon might be ascribed to the fact that the pressure and the surface conductivity of the void are increased by the internal PD within the void.

Fig. 10(c) shows the transformed shape of the PD pattern with time, for which the magnitude of PD has reached from 80pC to 2000pC due to the formation of electrical treeing as shown in Fig. 10(d)

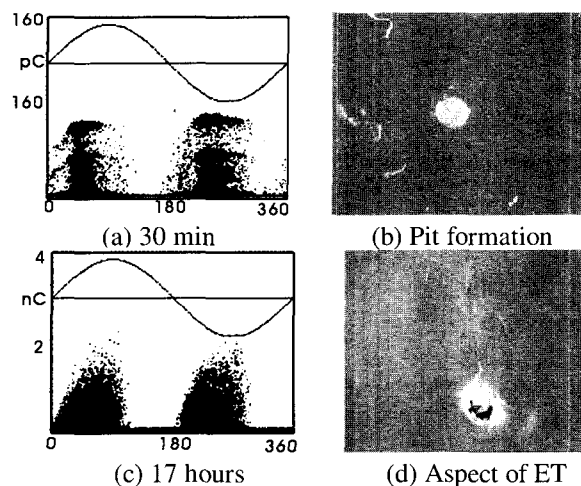
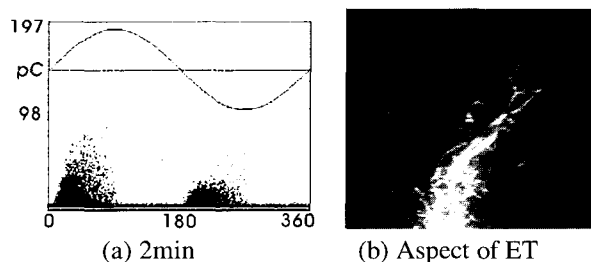
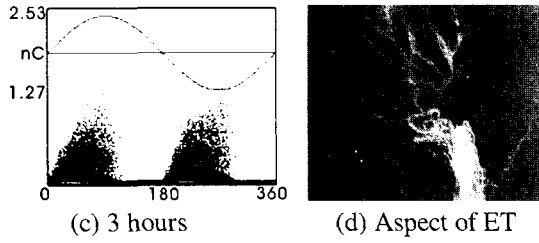


Fig. 10 Evolution of PD pattern for the void without silicone oil at  $3.5 E_{max}$ .

#### 3.2.3 Insulating fiber

Since the insulating fiber could be introduced into the interfaces due to the usage of cleansing paper together with cotton gloves, in this work, one 500  $\mu$ m insulating fiber with the diameter of 100  $\mu$ m was introduced. The PD pattern tends to be asymmetric at the very early stage of voltage application as shown in Fig. 11(a) where the magnitude of PD reaches up to 30pC. Fig. 11(b) shows the formation of electrical treeing produced from the fiber tip. As the degradation goes on, the aspect of the PD pattern is changed to be symmetric as shown in Fig. 11(c) with a few nC of PD. And, furthermore, a large electrical tree was observed in Fig. 11(d).





**Fig. 11** Evolution of PD pattern for the insulating substance without silicone oil at  $2.5E_{max}$ .

### 3.2.4 Scratch

Scratches can be inevitably formed by the use of sandpaper during the assemblage of the joint, and thus, its order of dimension is ranged to be a few micro-meters for its depth. In this study, a 10mm long scratch is formed along the direction of the electric field by use of #400 sandpapers. Instead of the aspect of the PD pattern which is unrecognizable as shown in Fig. 12(a), the magnitude of PD was measured after 10 minutes of voltage application as shown in Fig. 12(b). It could be remarked that the occasional PD occurrence in Fig. 12(b) is completely different from those by other defects. A large amount of PD was as shown in Fig. 12(c) due to the interfacial electrical treeing which is formed at the tip of the scratch in Fig. 12(d).

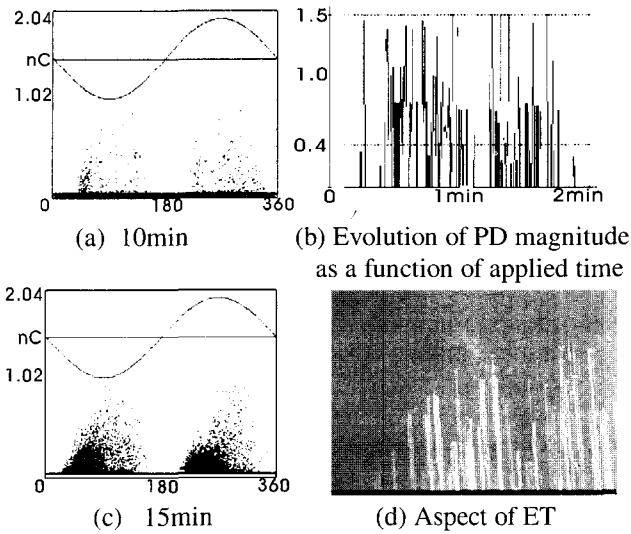


**Fig. 12** Evolution of PD pattern for the scratch without silicone oil at  $3.5 E_{max}$ .

### 3.3 PD pattern of the defects by chaotic analysis of partial discharge (CAPD)

Since the pulses are superimposed within finitely fixed phase windows of the applied voltage in the PRPDA method, it could be remarked that information about the correlations between consecutive pulses could hardly be deduced.

For this reason, a novel analytical method ‘‘CAPD’’ was proposed in our previous work [5]. The pulses related to PDs

are detected through continuous 7200 cycles of the applied voltage. Especially, the chaotic characteristics of three NDQs ( $P_t$ ,  $V_t$ , and  $T_t$ ) are verified by means of a 3-dimensional attractor in the phase space. In order to compare every piece of data with other one measured at different sequential moments, three parameters are normalized according to equations (1) through (6). The three parameters are magnitude of PD ( $P_t$ ), applied voltages when PD occurs ( $v_{vp}$ ) and differences of PD occurrence time ( $\Delta_t$ ). Afterwards, the one-dimensional time series of NDQs can be embedded in larger dimensional phase space (phase space reconstruction), in order to find the presence of converging bounded subset (strange attractor) [7]-[8]. Finally, in the 3-dimensional phase space, the specific characteristics of three NDQs are thoroughly examined in accordance with the nature of different defects.

$$v_t^* = \frac{V_t}{V_{tmax}}, \quad (-1 \leq v_t^* \leq 1) \quad (1)$$

$$p_t^* = \frac{P_t}{P_{tmax}}, \quad (0 \leq p_t^* \leq 1) \quad (2)$$

$$\Delta_t^* = \frac{\Delta_t}{T}, \quad (0 < \Delta_t^*) \quad \text{and} \quad T = \frac{1}{f} \quad (3)$$

$$V_t = v_t^* - v_{t-1}^*, \quad (-2 \leq V_t \leq 2) \quad (4)$$

$$P_t = p_t^* - p_{t-1}^*, \quad (-1 \leq P_t \leq 1) \quad (5)$$

$$T_t = \frac{\Delta_t^*}{\Delta_{tmax}^*}, \quad (0 \leq T_t \leq 1) \quad (6)$$

According to the application of our suggestion, 3-dimensional attractors are obtained from 3 main principal defects, as shown in Fig. 13, as their PD pattern. It could be deduced that each type of defects shows its typical pattern. By means of proper phase space reconstruction (embedding), it is possible to investigate the presence of chaotic characteristics, such as self-similarity and periodicity, by drawing an attractor based on the embedded time series, which can also be represented by a non-integer fractal dimension [7-8]. In consequence, it is preferable to ascertain the presence of a strange attractor, by means of appropriate phase space reconstruction. For this reason, it is necessary to determine the ‘‘embedding dimension( $Ed$ )’’ and ‘‘time delay ( $Td$ )’’ in order to obtain correct embedding. Accordingly, to compute  $Ed$  and  $Td$ , the False Nearest Neighbors (FNNP) method [9] and autocorrelation function were used, respectively [10]. Especially, if a computed  $Ed$  is larger than 10,  $Ed$  was assumed to be 10 in order to avoid overflow during calculation.

All of the computation was performed for each NDQs corresponding to three defects. These 3-dimensional strange attractors are shown in Fig. 13 using  $Ed$  and  $Td$  values in Table 2, respectively. It can be said that the presence of a strange

attractor in a phase space indicates the existence of fractal structures in its phase space. Furthermore, the strange attractor of  $Tt$  of each defect shows a very distinctive shape from the others. This distinctive shape will result in different quantitative properties such as dimension values, Lyapunov exponents' spectra and etc.

3-dimensional box-counting dimension ( $D_0$ : alternatively called the capacity dimension) can be computed by means of equation (7) for each  $NDQs$  trajectory for each defect under investigation.  $D_0$  is a very simple but convenient definition of the dimension set. However, it can definitely indicate whether the concerned attractor has a fractal orbit or not. For example, a point attractor has the value of 0 and a limit cycle attractor has the value of 1. If  $D_0$  is larger than 1 and a non-integer value, the concerning attractor could be considered as a fractal structure.

$$D_0 = \lim_{\epsilon \rightarrow 0} \frac{\ln M(\epsilon)}{\ln(1/\epsilon)} \quad (7)$$

$\epsilon$  : edge length of small cube in phase space

$M$ : the number of the boxes to cover all trajectories in 3-dimensional phase space

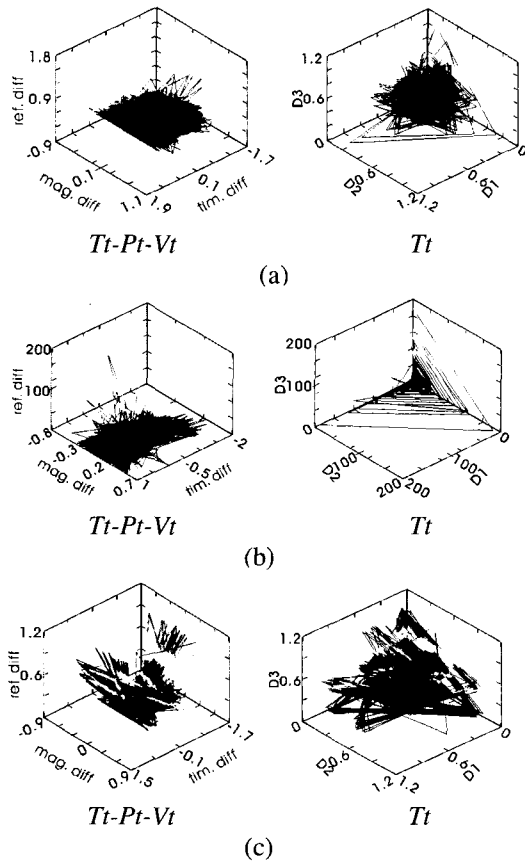


**Fig. 13** Strange attractors of  $Tt$ - $Pt$ - $Vt$  and  $Tt$  for conducting particle (a) void (b) insulating fiber (c)

In order to calculate the degree of divergences for the trajectories in Fig. 13, Lyapunov exponents spectra have also been investigated as functions of the given time inter-

val( $Td$ ) in Table 2 between two sequential center points. Among the different values of Lyapunov exponents corresponding to several given dimensions, the largest one ( $L_l$ ) is considered to determine the presence of chaos. For the positive one, the system could be considered to be divergent implying a chaotic system. Otherwise, the system would be converged [11]. Then, the Lyapunov dimension ( $D_L$ ) and K-S entropy ( $K$ ) can be calculated by means of equation (8) and equation (9), respectively [12].

$$D_L = j + \frac{\sum_{i=1}^j \lambda_i}{|\lambda_{j+1}|} \quad (8)$$

$$K = \sum_{i=1}^k \lambda_i \quad (9)$$

$j$ : index of largest positive integer of the sum of  $\lambda$

$i$ : index of  $\lambda$  by descending order

$k$ : index of the smallest positive  $\lambda$

Table 2 shows the values of the numerical indicators related to the 3 main parameters of  $NDQs$  corresponding to the different nature of the defects.

**Table 2** Numerical indicators for the defects

Defect	$NDQs$	Numerical indicators					
		$Td$	$Ed$	$Do$	$Ll$	$DL$	$K$
Conducting particle	$Tt$	27	10	0.4	3.26	10	5.49
	$Pt$	1	10	1.4	0.92	10	5.40
	$Vt$	17	10	0	5.21	9.20	2.79
Void	$Tt$	7	8	1.38	2.21	9.00	3.54
	$Pt$	1	9	1.58	0.97	7.96	0.55
	$Vt$	12	7	1.58	3.82	6.99	3.23
Insulating fiber	$Tt$	1	5	1.50	2.48	4.72	1.15
	$Pt$	1	6	1.53	2.57	4.98	0.66
	$Vt$	5	6	1.68	2.07	4.62	0.68

$NDQs$  : Normalize-Differenced Quantities ,  $Td$  : time delay

$Ed$  : embedding dimension

$Do$  : 3-dimensional box-counting dimension

$DL$  : Lyapunov dimension ,  $K$  : K-S entropy

$Tt$  : Normalized differences of timing between consecutive two pulses

$Pt$  : Differences in magnitude between consecutive normalized PD pulses

$Vt$  : Differences in amplitude between two normalized voltage values when PD take place

#### 4. Conclusions

From our experimental investigation, the following remarks can be deduced.

- In the case of interfacial defects, it could be suggested empirically to classify the degree of the evolution of the PD occurrence into two groups:  $PD_{GAP}$  and  $PD_{ET}$ . The former, of which the patterns could be distinguished from each other, depends on the nature of the

defects introduced into the test sample. However, the patterns of the latter are hardly distinguished from each other due to the electrical treeing propagated from the defects.

- Even though some further analysis is required for Table 2, it seems to be possible to identify the nature of the defects by the different values of the numerical indicators.
- Each defect has shown its particular characteristics in its PD pattern by two methods of analysis: PRPDA and CAPD, respectively. And, moreover, the latter allows us to identify the nature of the defects more distinctively.

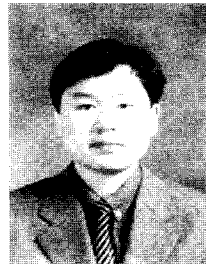
However, further works are planned to investigate the suitability of the CAPD method for its on-site application and to deduce the possible correlations between the chaotic analysis and PD occurring process. Furthermore, elaborated investigations are necessary to provide quantitative indicators for a pattern recognition algorithm combined with the CAPD method, in connection with the nature of defect.

### Acknowledgement

This research was supported by Research Center for Electronic Materials & Components (EM&C) and LG Cable co. Ltd, KOREA.

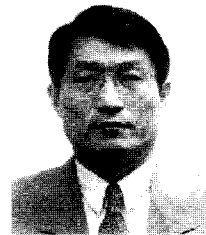
### References

- [1] T. Tanaka, M. Nagao, Y. Takahashi, A. Miyazaki, M. Okada, Y. Yamashita, "Dielectric characteristics in prefabricated joints of extra-high voltage XLPE cables" CIGRE Session 2000, Group 15-206, 2000.
- [2] E. Gulski, W. Boone, E.R.S. Groot, J. Pellis and B.J. Grotenhuis, "Knowledge Rules Support for CBM of Power Cable Circuits", Session 15-104, CIGRE, 2002.
- [3] Hiroshi Yoshida and Zhihai Tian and Masayuki Hikita and Hiroyuki Miyata, "Study on the time evolution of partial discharge characteristics and interfacial phenomena of simulated XLPE cable joint", Electrical Insulating Materials, Proceedings of International Symposium, D2-3, pp. 501-504, 1998.
- [4] B.A. Fruth, D.W. Gross, "Partial discharge signal generation transmission and acquisition" IEE Proc.-Sci. Means. Technol., Vol. 142, No. 1, January 1995.
- [5] Y.S. Lim, J.Y. Koo, J.S. Lee, W.J. Kang, "Chaotic analysis of Partial Discharge, A novel approach to identify the nature of PD source", Annual Report Conference on Electrical Insulation and Dielectric Phenomena, pp. 324-328, 2001.
- [6] Robert Ross and Mark Megens, "Aging of interfaces by discharging", Properties and Applications of Dielectric Materials, Proceedings of the 6th International Conference, vol. 1, pp. 227 -230, June 2000.
- [7] K. Alligood, T. Sauer and J. Yorke, *CHAOS - An introduction to dynamical systems*, Springer, 1996.
- [8] D. Kaplan and L. Glass, *Understanding Nonlinear Dynamics*, Springer, 1995.
- [9] Edward Ott, Tim Sauer and James A. Yorke, *Coping with chaos-Analysis of chaotic data and the exploitation of chaotic systems*, John Wiley & Sons Inc., 1994.
- [10] Mathew B. Kennel, Reggie Brown and Harry D. I. Abarbanel, "Determining embedding dimension for phase-space reconstruction using a geometrical construction", Physical Review A, Vol. 45, pp. 3403-3411, 1992.
- [11] A.M. Albano, J. Muench, C. Schwarts, A.I. Mess and P.E. Rapp, "Singular-value decomposition and the Grassberger - Procaccia algorithm", Physical Review A., Vol. 38, pp. 3017-3026, 1988.
- [12] Andrew M. Fraser and L. Swinney, "Independent coordinates for strange attractor from mutual information", Physical review A, Vol. 33, No. 2, pp. 1134-1140, 1986.



**Jeon-Seon Lee** was born in 1968 in Korea. He received his B.S degree and M.S degree from Hanyang University, Seoul, Korea in 1994 and 1998 respectively. Since 1998 he has been in the Ph.D. course at Hanyang University in the area of insulating materials. His research interest is in high frequency partial discharge de-

tection for the diagnosis of underground power cable systems.



**Ja-yoon Koo** was born in 1951 in Korea. He received his B.S. degree from Seoul National University, Seoul Korea in 1975, M.S. degree from ENSEEISH, Toulouse, France in 1980 and Ph.D. in High Voltage insulating Dielectrics, from ENSIEG. Grenoble, France in 1984. He joined the Research Center of the Electric-

ity of France (EDF), at the High Voltage and High Power Laboratory after his dissertation in France and then worked for the Korea Advanced Institute of Science and Technology, Seoul, Korea. He has been with the Department of Electrical Engineering, Hanyang University, Ansan, Korea since 1988 as a professor and is head of the Research Center for Electronic Materials and Components in Hanyang University. His main research activities are in the areas of the New Dielectrics used for High Power Engineering, Diagnosis of Electric Power Apparatus and the Protection of High Voltage Network System.